Click Here for Full Article

Searching for microbial life remotely: Satellite-to-rover habitat mapping in the Atacama Desert, Chile

K. Warren-Rhodes,[1] S. Weinstein,[2] J. Dohm,[3] J. Piatek,[4] E. Minkley,[2] A. Hock,[5] C. Cockell,[6] D. Pane,[2] L. A. Ernst,[2] G. Fisher,[2] S. Emani,[2] A. S. Waggoner,[2] N. A. Cabrol,[7] D. S. Wettergreen,[8] D. Apostolopoulos,[8] P. Coppin,[9] E. Grin,[7] Chong Diaz,[10] J. Moersch,[4] G. G. Oril,[8] T. Smith,[8] K. Stubbs,[8] G. Thomas,[11] M. Wagner,[8] and M. Wyatt[3]

Received 3 August 2006; revised 14 April 2007; accepted 1 June 2007; published 29 August 2007.

[1] The Atacama Desert, one of the most arid landscapes on Earth, serves as an analog for the dry conditions on Mars and as a test bed in the search for life on other planets. During the Life in the Atacama (LITA) 2004 field experiment, satellite imagery and ground-based rover data were used in concert with a 'follow-the-water' exploration strategy to target regions of biological interest in two (1 coastal, 1 inland) desert study sites. Within these regions, environments were located, studied and mapped with spectroscopic and fluorescence imaging (FI) for habitats and microbial life. Habitats included aqueous sedimentary deposits (e.g., evaporites), igneous materials (e.g., basalt, ash deposits), rock outcrops, drainage channels and basins, and alluvial fans. Positive biological signatures (chlorophyll, DNA, protein) were detected at 81% of the 21 locales surveyed with the FI during the long-range, autonomous traverses totaling 30 km. FI sensitivity in detecting microbial life in extreme deserts explains the high percentage of positives despite the low actual abundance of heterotrophic soil bacteria in coastal ($<1-10^4$ CFU/g-soil) and interior ($<1-10^2$ CFU/g-soil) desert soils. Remote habitat, microbial and climate observations agreed well with ground-truth, indicating a drier and less microbially rich interior compared to the relatively wetter and abundant biology of the coastal site where rover sensors detected the presence of fog and abundant surface lichens. LITA project results underscore the importance of an explicit focus by all engineering and science disciplines on microbially relevant scales (mm to nm), and highlight the success of satellite-based and 'follow-the-water' strategies for locating diverse habitats of biological promise and detecting the microbial hotspots within them.

Citation: Warren-Rhodes, K., et al. (2007), Searching for microbial life remotely: Satellite-to-rover habitat mapping in the Atacama Desert, Chile, *J. Geophys. Res.*, *112*, G04S05, doi:10.1029/2006JG000283.

[1]NASA Ames Research Center, Moffett Field, California, USA.
[2]Molecular Biosensor and Imaging Center, Carnegie Mellon University, Pittsburgh, Pennsylvania, USA.
[3]Department of Hydrology and Water Resources, University of Arizona, Tucson, Arizona, USA.
[4]Department of Earth and Planetary Sciences, University of Tennessee, Knoxville, Tennessee, USA.
[5]Department of Earth and Space Sciences, University of California, Los Angeles, California, USA.
[6]Planetary and Space Sciences Research Institute, Open University, Milton Keynes, UK.
[7]SETI Institute, Mountain View, California, USA.
[8]Robotics Institute, Carnegie Mellon University, Pittsburgh, Pennsylvania, USA.
[9]Eventscope, Carnegie Mellon University, Pittsburgh, Pennsylvania, USA.
[10]Universidad Católica del Norte, Antofagasta, Chile.
[11]Department of Mechanical and Industrial Engineering, University of Iowa, Iowa City, Iowa, USA.

Copyright 2007 by the American Geophysical Union.
0148-0227/07/2006JG000283$09.00

1. Introduction

[2] In preparation for future Mars science missions, the 'Life in the Atacama' (LITA) project advanced robotic capabilities for long-distance traverse and the detection and characterization of life in extreme environments. The project consisted of a 2003 preliminary field test, followed by science and engineering campaigns in 2004 and 2005. With each successive field campaign, progressively more challenging goals and methods evolved and were tested to hone rover and science abilities to map habitats and identify biological signatures in terrestrial deserts as analogs for the conditions and potential life (past or present) on Mars [*Cabrol et al.*, 2007].

[3] The Atacama Desert in Chile was selected for all LITA field campaigns (Figure 1) because it represents a unique Mars analog study environment and test location for astrobiology exploration rovers [*Sutter et al.*, 2002; *Navarro-González et al.*, 2003; *Quinn et al.*, 2005; *Wettergreen et al.*, 2005; *Warren-Rhodes et al.*, 2006]. Much of this temperate

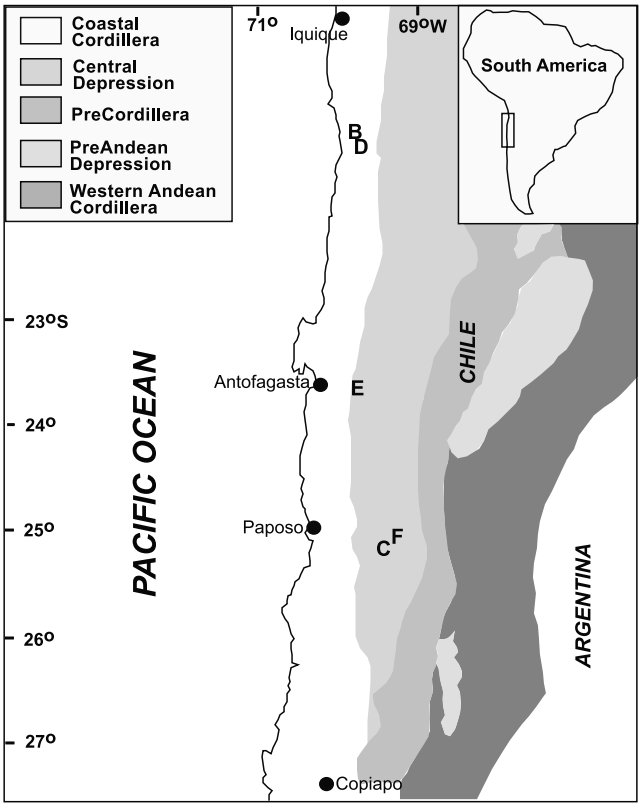

Figure 1. LITA site locations (adapted from *Riquelme et al.* [2003]) within major longitudinal physio-geographical units (coastal to Andean) in the Atacama Desert, Chile.

desert, which covers the northern one-third of Chile (18°S to 28°S), is hyperarid, and these extremely dry conditions have persisted ca 15–25 Mya [*Houston and Hartley*, 2003; *Dunai and González-López*, 2005]. Its interior 'core' (~24–25°S, 69–70°W) receives ≪5 mm mean annual rainfall and many locations experience years to decades with no significant rainfall [*Miller*, 1976; *McKay et al.*, 2003; *Warren-Rhodes et al.*, 2006]. Extremely dry conditions also exist at the microbial scale, where in the Atacama's core microclimate sensors have recorded an average of <400 hrs of liquid water yr^{-1} (maximum) available for bacteria beneath rocks and in upper (>10 cm) soils [*Warren-Rhodes et al.*, 2006]—the lowest of any desert studied. Outside the core, higher water availability supports greater plant and microbial abundance and diversity—from cactus and lichen populations exploiting coastal fog to rich desert ecosystems in humid inland sites (south of ~27°) and near the eastern Andes [*Rundel et al.*, 1991; *Latorre*, 2002; *Latorre et al.*, 2003; *Drees et al.*, 2006]. This habitat diversity and wide range of moisture conditions within the Atacama's geographical boundaries enhances its desirability as a test bed for designing and testing rovers that will assist in the search for life on other planets.

[4] This paper focuses on the 2004 LITA campaign, where overall science objectives were to locate microbial life and map habitats in two major climatic zones (coastal, interior). Within each zone, a single site was chosen and investigated. In 2004, Site B was selected to represent a relatively 'wet' location (characterized by coastal fog) in the Atacama, whereas Site C was chosen as an extremely 'dry' (interior desert) environment. These climate classifications, along with the coastal nature of Site B (the Pacific coast was visible in pre-traverse satellite imagery), were the only information science team members had regarding the particular LITA field locations until the study's conclusion and ground-truth field trip in Jan. 2006. Consequently, and in order to retain a sense of the original biological findings gleaned solely from remote data analysis during the field campaign, this paper limits references to external literature (which was prohibited for team members until 2006) or previous work at the sites to only those discussions concerning ground-truth data.

[5] Logistically, an interdisciplinary team of scientists (biologists, ecologists, geologists and spectroscopists) worked remotely from Carnegie Mellon University, PA to direct an automated rover to study and sample within the two field sites in the Atacama Desert. Each day (sol), data collected in-situ by the rover was downloaded, analyzed and used by the remote science team to assess the environment surveyed, generate and test hypotheses and build the subsequent day's sampling plan. Individual site studies lasted ~1 week [*Cabrol et al.*, 2007]. Our paper presents a detailed look at the ecological results and overview of the microbiological findings for the LITA 2004 field experiment. Overall, biological project milestones for the 2004 field campaign included (1) development of an on-board rover microscopic and fluorescence imaging system that successfully detected biota during daylight operations at both coastal and interior Atacama desert sites; (2) identification (from satellite imagery) and study of regions of biological interest, and confirmation of the presence of life within those environments; (3) in-depth mapping, including both biotic and abiotic (mineralogy, geology, climate) characteristics, of habitats surveyed during long-range traverses. For in-depth analysis of the fluorescence methods and results, the reader is directed to S. Weinstein et al. (Application of pulsed-excitation fluorescence imager for daylight detection of sparse life in tests in the Atacama Desert, submitted to *Journal of Geophysical Research*, 2007, hereinafter referred to as Weinstein et al., submitted manuscript, 2007), while additional information on the LITA project and science results is summarized in companion papers elsewhere [*Cabrol et al.*, 2007], including rover instrumentation and mineralogy (J. Piatek et al., Surface and subsurface composition of the Life in the Atacama field sites from rover data and orbital image analysis, submitted to *Journal of Geophysical Research,* 2007, hereinafter referred to as Piatek et al., submitted manuscript, 2007).

2. Approach and Methods

2.1. Rover Instrumentation

[6] Rover instrument capabilities included a visible/near-infrared (VIS/NIR) spectrometer to identify mineralogy and locate chlorophyll signatures; a thermal infrared (TIR) spectrometer (human-operated during LITA), which also collects information on mineralogy; workspace imagers (WI) and stereo panoramic imagers (SPI), which obtain macroscale and microscale imagery and furnish contextual ecology and geology (km to cm); and a microscopic and fluorescence imager (FI) (Table 1). Microscopic images

Table 1. Table of Acronyms Used in the LITA Project

Acronyms	Definition
LITA	'Life in the Atacama' project;
VIS/NIR (VNIR)	Visible/near-infrared spectrometer (see Piatek et al., submitted manuscript, 2007);
TIR	Thermal infrared spectrometer (see Piatek et al., submitted manuscript, 2007);
WI	Workspace imager;
SPI	Stereo panoramic imager;
FI	Microscopic and fluorescence imager;
RGB	Red-green-blue (images from the microscopic imager);
DEM	Digital elevation model;
IKONOS	Commercial earth observation satellite that provides multi-spectral high resolution imagery (see Piatek et al., submitted manuscript, 2007);
ASTER	Advanced spaceborne thermal emission and reflection radiometer (see Piatek et al., submitted manuscript, 2007);
CFU	Colony-forming units.

from the FI camera are high-resolution RGB, with a field of view of 10 cm $\times$ 10 cm and 223 μm/pixel resolution. The WI image field of view is $\sim$1.5 m $\times$ 1.3 m, while the SPI imager, composed of three Sony DFW-SX900 12-bit color cameras (400–700 nm sensitivity), has a 21.9° $\times$ 15.9° field-of-view and 1280 $\times$ 960 pixel resolution, which results in a 0.28 mrad/pixel resolution. Macroscale climate conditions were also recorded during the field campaign by a stationary Campbell Scientific, Inc.® meteorological station, including rainfall, wind speed and direction, solar radiation, and air temperature and relative humidity. In 2005, on-board environmental sensors were added to complement the weather station data and account for the rover's extended mobility. For a detailed overview and specifications of the rover instrument payload, the reader is referred to *Cabrol et al.* [2007], Piatek et al. (submitted manuscript, 2007), and Weinstein et al. (submitted manuscript, 2007).

[7] Fluorescence (emission of light by molecules upon illumination) is a sensitive analytical method that has been used to detect microorganisms in the laboratory and field. Certain biological molecules, such as the chlorophyll contained in cells of photosynthetic bacteria, are intrinsically fluorescent, and numerous investigators have used chlorophyll and phycobiliprotein fluorescence for detection of such microorganisms [*Shapiro*, 2003]. Others have used ultraviolet lasers to excite endogenous fluorophores such as tryptophan in proteins, NADH, flavins and flavoproteins that emit in the near-UV and blue regions of the spectrum [*Shapiro*, 2003]. Additionally, exogenously added fluorescent probes that target nucleic acids, proteins, lipids and carbohydrates (the four classes of organic compounds possessed by all living organisms) are also valuable for visualizing microorganisms. For example, DAPI staining of DNA is widely used [*Shapiro*, 2003], and other fluorogenic probes have been designed commercially (e.g., Syto BC, Sypro Red) and in biological laboratories to detect DNA, proteins, lipids, membrane potential changes, and other specific targets. The Molecular Probes Handbook describes many of these probes and their targets (Invitrogen.com).

[8] The microscopic and fluorescence imaging system (FI) developed for the LITA rover detects microbial communities through the use of such targeted fluorescent probes for DNA, protein, lipids and carbohydrates and via chlorophyll directly. The primary goal in development of the FI system was to deploy an imager capable of detecting fluorescence signals during autonomous rover exploration in daylight [*Cabrol et al.*, 2007], which required band-pass filters and a high sensitivity camera to image in sunlight. The FI consists of a Roper CoolSNAP cooled CCD camera, 12-bit, 1392 $\times$ 1040 pixel array (used center 1024 $\times$ 1024 array) at 6.45 μm pixels, a Schneider Xenoplan 1.4/17 lens, a fiber bundle light delivery system, and two filter wheels, one for emission and one for excitation. The FI instrument is positioned under the belly of the rover and can be moved 25.5 cm along the z-axis and 67.75 cm along the x-axis. Illumination is obtained with a PerkinElmer FX4400 flashlamp, delivering pulses at 20 μsec/flash [*Fay*, 1982; *Ford and Leather*, 1984; *Kim et al.*, 2003; *Norikane and Kurata*, 2001]. The camera is synchronized with the flash, permitting the detection of fluorescence over diffuse ambient light.

[9] Color (RGB) microscopic images are created with the FI by imaging with 630 nm (red), 535 nm (green), and 470 nm (blue) band-pass filters using full spectrum illumination from the underbody flash lamp. Fluorescence images are acquired by flash-no flash subtraction. Chlorophyll's natural fluorescence is imaged by 450 nm (blue) or 540 nm (green) excitation and 740 nm (infrared) detection. For DNA, proteins, lipids and carbohydrates, dilute dyes are applied in-situ to the sample surface. Sensitivities for biota varied and depended upon the relative efficiency of dye penetration to reach the targeted biomolecules, with detection limits of 1×10^6 cells/mm^2 biofilm imaging area in laboratory experiments simulating Atacama Desert conditions and FI field protocols (Weinstein et al., submitted manuscript, 2007). For a full list and discussion of the fluorescent dye probes, excitation and emission bands that interrogated the probes, dye protocols and issues (e.g., poor penetration in lichens, wind effects on sprayer) encountered during the LITA project, see Weinstein et al. (submitted manuscript, 2007). The DNA and protein probes were deployed in 2004 and the full suite of probes was used by 2005. Dye application was manual in 2004, with a sample requiring $\sim$1 hr to complete, but became automated and streamlined to $\sim$35 minutes per sample by 2005.

2.2. Habitats and Microbiology

[10] Rover instruments and environmental sensors were deployed during the 2004 LITA field campaign to detect and characterize (1) the habitats surveyed during the traverse, and (2) the signatures of biological, mainly microbiological, life within such habitats. In this paper, a 'habitat' is defined as a place where a microorganism(s) may live, and

it encompasses an environment's abiotic features, including geology, geomorphology, topography, hydrology, climate, chemistry and mineralogy. Habitats may occur at many scales, such that a 'salt habitat' can be a 10 km-wide hypersaline deposit, a 1 m-high gypsum boulder, or a 1-cm to 1-μm halite crystal. Prior to the field experiment, four main classes of habitats (not mutually exclusive) were hypothesized to exist in the Atacama Desert: (1) *Rock habitats*, including outcrops, alluvial fans, hillslopes, and desert pavements (surface soils mantled by gravels); (2) surface and near-surface *soil habitats*; (3) *saline habitats*, including soils and rock materials (aqueous sedimentary deposits such as evaporites or exposed saline-rich fluvial deposits) in basins and topographic lows (e.g., hypersaline lakes); and (4) *extant and paleo-aqueous habitats*, including seeps (hydrothermal and/or groundwater systems), ponding in topographic lows (playas), ancient lakes (Salar Grande) or areas with atmospheric moisture embankments. A wide array of microbial communities, ranging from lithophytic [*Friedmann and Galun*, 1974; *Nienow and Friedmann*, 1993] to thermophilic to halophilic, could occupy the above habitats, including eukaryotic and prokaryotic populations that support both photosynthetic (possessing chlorophyll or bacteriochlorophyll, e.g., lichens and cyanobacteria) and non-photosynthetic members (e.g., heterotrophic bacteria).

[11] During the 2004 field campaign, a preliminary scheme was devised to assess biological 'diversity' at locales sampled by the rover. Assessments were made solely based on rover data and included visual evidence of macroscale (e.g., plants in SPI image) and microscale (e.g., lichens in FI RGB image) biology coupled with information gleaned from fluorescence results. In 2004, FI images were analyzed in terms of four biosignature channels (visible, chlorophyll, DNA, protein), with each channel receiving a 'negative' (no positive signal), 'positive' (strong positive signal), or inconclusive (e.g., possible sunlight effects) rating. Samples with multiple, converging positive signals (e.g., DNA + protein) were viewed as stronger evidence for the presence within a habitat of life than a single positive signal (e.g., DNA only). When comparing a locale or site's biological 'diversity,' a simple scheme was used that defined diversity as being comprised by the presence/absence of four components (a posteriori): 1) higher plants (no macrofauna were observed during the field experiment), 2) eukaryotic lichens, 3) prokaryotic photosynthetic microorganisms (e.g. detected by presence of chlorophyll, exclusive of lichens) and 4) non-photosynthetic microorganisms (e.g., positive DNA signal). A locale with three components present would thus be concluded to have higher relative biological diversity than a locale exhibiting only 2 components. Unless otherwise noted, biological/microbial diversity in this paper refers only to this simple definition determined by rover presence/absence data. A more elaborate rating methodology to compare biological findings across samples and locales was developed—as experience and data volume progressively increased—in 2005 [*Warren-Rhodes et al.*, 2007; Weinstein et al., submitted manuscript, 2007].

[12] At the conclusion of the LITA project (2006), complementary data for microbial abundance and diversity obtained through other methods for samples collected (by a second science field team) at each rover locale during the 2004 field test were released to the remote science team. Briefly, during the 2004 field campaign, a thin layer (~0.5–1 cm depth) of exposed soil in each 10 × 10 cm area imaged by the rover was collected with sterile scoops and placed in a sterile Whirlpak® bag. All samples (n = 23 from 15 Site B locales; n = 15 from 11 Site C locales) were kept at ambient temperature until return to the laboratory in Pittsburgh and analysis. Laboratory culturing of sample soil extracts on 1/10 strength Plate Count Agar (PCA) medium was used to investigate each locale's aerobic heterotrophic bacterial abundance [*Navarro-González et al.*, 2003; *Lester et al.*, 2007], with most probable number (MPN) enumerations performed to estimate the number of colony-forming units per gram of soil (CFU/g-soil) [*de Man*, 1975; *Navarro-González et al.*, 2003]. Initial MPN tubes (in triplicate) contained 1 g soil in 5.5 ml culture medium and were agitated on a wrist action shaker 30 min. prior to the dilution series [*de Man*, 1975]. Culture tubes were incubated at room temperature for 1 week and three weeks. Aliquots from culture tubes that developed turbidity were plated onto 1/10 strength PCA, and growth was then streaked to isolate single colonies for further identification of bacterial diversity through gene sequencing.

[13] Additional characterization of the microbial communities encountered at a locale during the rover traverse was obtained through culture-independent (molecular) methods, but because such in-depth assessments were beyond the original main scope of the project, in 2004 efforts were concentrated on rover locales within a single site (Site C). All isolated colony types from each Site C locale were identified by nucleotide sequence determination of a portion of their 16 S ribosomal RNA gene. Purified single colonies of the isolates were inoculated into liquid R2A medium and grown as shake flask cultures at room temperature. [The growth medium was switched to R2A because some isolates would not grow on 1/10th PCA medium unless they were co-cultured in the presence of another isolate (i.e. on the same plate).] Cells were collected by centrifugation, and genomic DNA was extracted from the cell pellets by using a GNOME DNA kit (Qbiogene, Carlsbad, CA) and following the manufacturer's instructions. A 1 to 5 dilution of the extracted DNA was used for PCR amplification of a portion of the gene for 16 S ribosomal RNA according to the conditions described by *Edwards et al.* [1989]. The primers 341F (5′-CCTACGGGAGGCAGCAG-3′) targeting *E. coli* positions 341–357 and 928R (5′-CCCCGTCAATTCCTTTGAGTTT-3′) targeting E. coli positions 928–907 were used for the amplification of a middle 40% of the 16 S rDNA gene [*Edwards et al.*, 1989] that includes variable regions that are useful diagnostics for species identification. Successful amplification of the target region was confirmed by electrophoresis of the PCR reaction products on a 0.8% agarose gel in TAE buffer (Tris/acetate/EDTA) and visualization of the ethidium bromide stained bands with a UV light. In those cases where there was a single product of the correct size, the PCR amplified products were purified directly from the reaction mixtures with a QIAquick PCR purification Kit (QIAGEN, Inc., Valencia, CA) according to the manufacturer's instructions. Where the PCR product had additional bands, the entire PCR reaction mixture was run on a 0.8% agarose gel and the correct molecular weight band was excised from the gel with a razor blade. The DNA

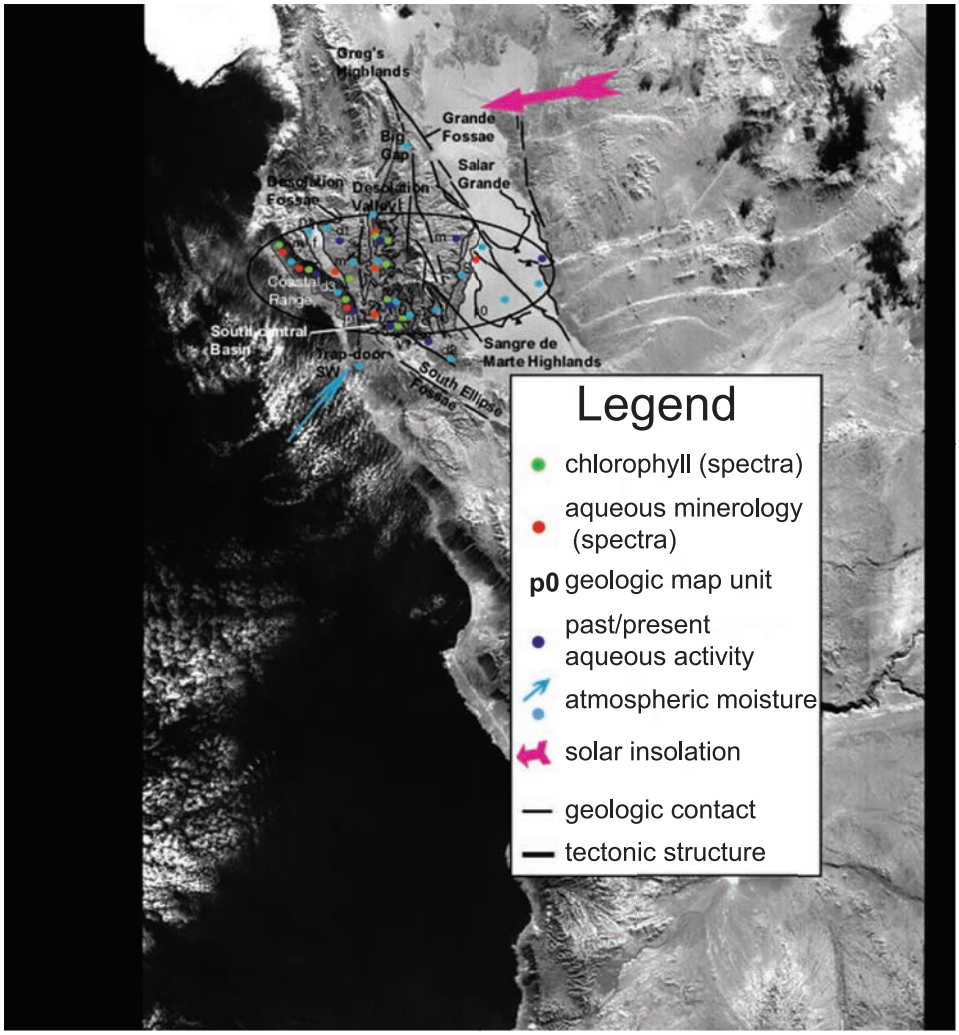

Figure 2. Schematic map of Site B showing pre-traverse, satellite-based reconnaissance, including the landing ellipse, geologic map units, and dots that represent regions of biological interest based on four main selection criteria (see Table 2). Geologic map units include m (mountain-forming materials), d (dissected materials, d1, d2 and d3), s (scalloped terrain) and f (fan materials). Contacts (solid thin lines or dashed, if approximately located), faults (solid thick lines, dotted where buried) and scarps (solid thick lines with arrows) are also shown. Dark blue dots represent regions that record ancient and/or extant aqueous activity (e.g., valley networks or drainage basins). Light blue dots and blue arrows indicate possible influence by atmospheric moisture (clouds, fog embankments). Orange-red and green dots highlight spectroscopic mineralogical signatures of aqueous activity (e.g., carbonates) or chlorophyll, respectively. Pink arrow indicates general direction of solar insolation.

was then extracted from the gel band using a GENECLEAN II Kit (BIO 101, Inc., La Jolla, CA). DNA sequences were determined at the Automated DNA Sequencing Facility operated by the Department of Molecular Genetics and Biochemistry, University of Pittsburgh, Pittsburgh, PA. Aliquots of the purified, amplified 16 S rDNA PCR products were separately combined with each of the PCR primers, using the amounts specified on the Web site of the DNA sequencing facility. The raw data received from the sequencing facility was aligned as sequence and complementary sequence to give a composite two-stranded sequence, typically 500 base pairs in length. The 16 S rDNA sequences were then submitted electronically to the Ribosomal Database Project Web site to perform sequence match and phylogenetic analyses [*Maidak et al.*, 2000].

[14] It should be noted that each of the above approaches for assessing biological abundance and diversity, whether it is rover-acquired visual and fluorescence imagery, culturing, or phylogenetic analysis, likely result in an incomplete characterization of the 'true' abundance and diversity at a locale. Fluorescent dyes have difficulty penetrating particular types of microorganisms in-situ (e.g., lichens (see Weinstein et al., submitted manuscript, 2007)); culturing has been known to underestimate microbial abundance by 1 to 2 orders of magnitude; a vast majority of microbial diversity has proven refractory to cultivation; and the efficiency of DNA extraction varies widely [*Amman et al.*, 1995; *Hartmann et al.*, 1997; *Miller et al.*, 1999; *Tien et al.*, 1999; *Lloyd-Jones and Hunter*, 2001; *Kaeberlein et al.*, 2002; *Zengler et al.*, 2002; *Li et al.*, 2004]. Exhaustive

Table 2. Selection Criteria for Orbital-Scale Regions of Biological Interest

Criterion	Selected Indicators
Biosignatures	Spectroscopic-based chlorophyll signatures based on VNIR spectra from IKONOS satellite imagery (green dots in Figure 2)
Mineralogy	Spectroscopic-based carbonate signatures based on TIR satellite spectra (indication of aqueous activity; orange dots in Figure 2)
Water-associated (geology, geomorphology, hydrology)	Landforms, which mark past/present aqueous activity, such as valley networks, sapping channels, and drainage basins that may have ponded water (dark blue dots in Figure 2), and topography that influences the flow of atmospheric water vapor (e.g., topographic highs such as promontories) and/or where incursions of marine fog might bank (consistent with 'follow the water' strategy; light blue dots in Figure 2).
Habitats	Environments and habitats (identified from field experience to hold significant potential for life), such as alluvial fans with quartz-rich desert pavement (e.g., favorable for photosynthetic communities). These environments were also identified by satellite based reconnaissance, including TIR spectral maps that indicated the presence of volcanics, quartz, evaporites (e.g., Salar Grande, which was identified by remote operations during the 2003 LITA field test).

inventories of microbial abundance and diversity thus remain challenging [*Hughes et al.*, 2001].

2.3. "Orbit-to-Ground" Science Sampling Strategy

[15] When presented with pre-traverse satellite imagery of a site within which a rover will likely land (the 'landing ellipse', Figure 2), the first, and arguably one of the most important decisions, a remote science team must make is where to sample. This requires not only identification of the most promising areas of biological interest within the landing ellipse but also prioritization of those areas for investigation. In 2004, the overall LITA science sampling (exploration) strategy adopted was not chosen a priori but evolved from a distillation of the team's knowledge, experience and work methods. It encompassed two distinct phases, each characterized by different analytical scales, work modes and processes. The first phase focused on the "regional" scale (i.e., $\geq$30 m^2, the approximate size of a DEM pixel) and comprised initial selection of regions of astrobiological interest as gleaned from satellite imagery. The second phase centered on the "local" scale on the ground, corresponding to a panoramic image returned by the rover SPI camera, which then became the basis for sampling activity. The science team shifted back and forth continuously between these two phases/scales, reflecting iterations between short-term (daily sol) and long-term (next sol or further) temporal planning horizons.

2.3.1. Selection of Regions of Biological Interest From Satellite Imagery

[16] The primary objective of pre-traverse, satellite-based reconnaissance is to identify promising regions of interest to search for microbial life remotely by rover. In this initial phase, the science team used (1) orbital digital elevation model (DEM) and VIS/NIR images (IKONOS satellite imagery, 1 m/pixel resolution; ASTER VIS/NIR imagery, 15 m/pixel) to assess geomorphology and detect regions with chlorophyll, and (2) TIR spectra (ASTER imagery, 90 m/pixel) to construct topographic profiles and geologic and spectral maps. The pre-traverse map created by the science team with regions of interest for Site B is shown in Figure 2 and explained below. The map's functions were to highlight regions of interest with particular promise for containing life, to anchor and focus the science team's priorities and rationale during the field experiment, and to guide short- and long-term traverse planning.

[17] Orbital-based identification and selection of regions of interest was accomplished via several general considerations. One such consideration was the targeting of environments influenced by aqueous activity—a *'follow the water' strategy* parallel to one employed by *NASA* [2006] in the search for life on Mars (and other planets and celestial bodies). In addition to large-scale effects of water activity (including valley networks, sapping channels, topographic basins), cloud movements, the flow of fog and possible rainshadow effects could also be determined from orbital imagery. Mineralogies associated with aqueous activity, as well as regions postulated from orbital and spectral data to contain promising biological habitats, such as evaporite deposits or playas (also an element of a follow-the-water strategy), were also targeted. Finally, the presence of key biomarkers, such as chlorophyll, guided regional selection. Prokaryotic oxygenic photosynthesizers, which possess chlorophyll (as do plants, lichens, and soil crusts), are model organisms to test life detection technologies because of their readily demonstrable biomarkers and ease of identification. (However, we recognize that, as a group, cyanobacteria specifically may be an unlikely target on Mars.) In summary, selection criteria included 'mineralogy', 'water-associated', 'habitat' and 'biosignatures' categories (Table 2). Convergence of one of more criteria within a region resulted in a high priority for its exploration.

2.3.2. Ground-Based Habitat Mapping and the Search for Life

[18] Rather than ground-based targeting—i.e., 'pre-selecting' promising individual rocks, soils, etc. based on predetermined criteria—FI samples were chosen within regions of interest by distance (e.g., a request to take an FI every 30 m) or by other considerations, such as an end-of-sol sample. This type of sampling strategy was adopted for several reasons. First, it is currently unknown on Mars (or other planets and celestial bodies) whether extant or extinct microbial populations would be distributed randomly or non-randomly within environments. Because the conditions creating non-random microbial spatial distributions on Mars may not be deducible a priori (i.e., based on Earth analogs), random sampling may have an equal or larger probability of

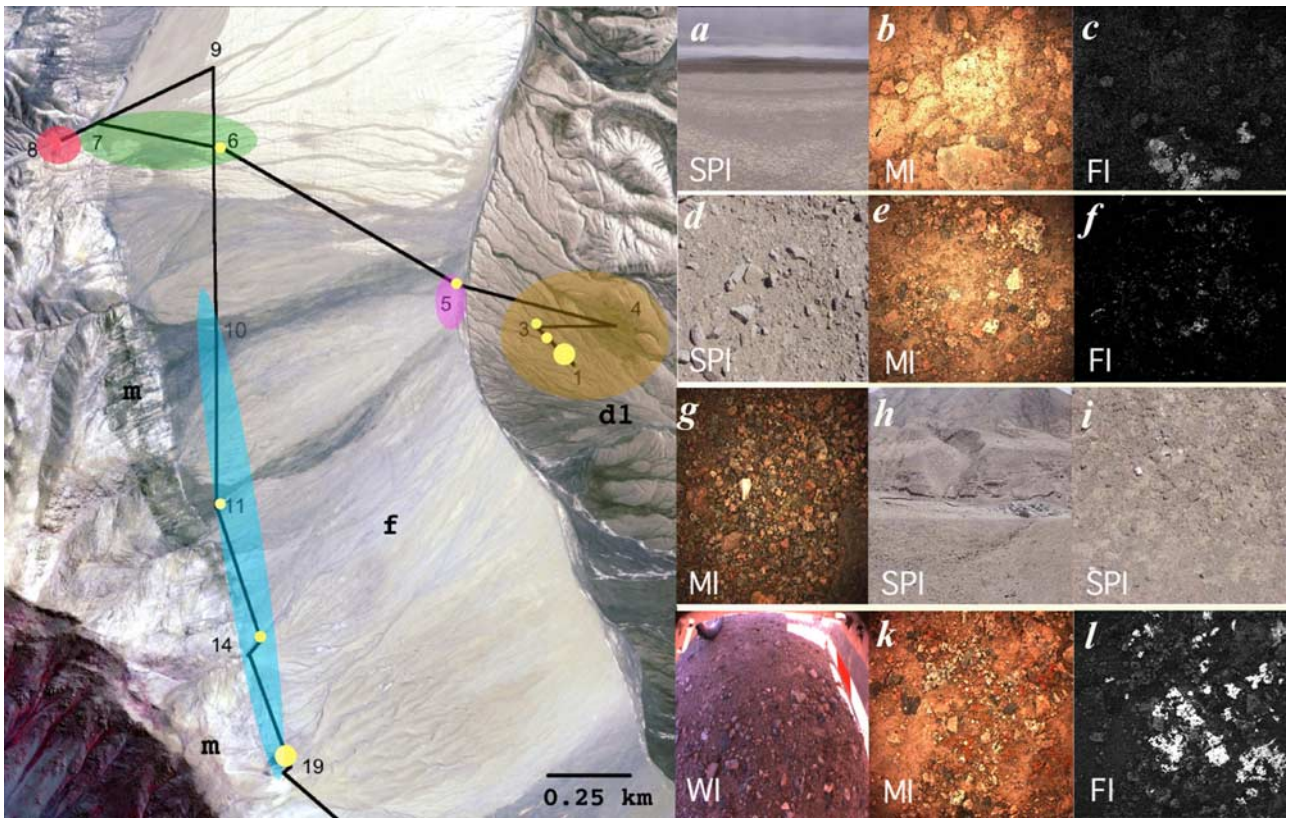

Figure 3. Schematic map showing locales sampled, geologic units and habitat zones for Site B. Distinct habitat zones were identified from SPI and FI data (visible and fluorescence) assessments during the traverse and included: desert pavement/alluvial fan habitats (brown, locales 1–4; blue, locales 10–19), contact and drainage-type habitats (pink, locale 5; red, locale 8) and transition zones (green, locales 6–7). The colored ovals are shown to highlight each habitat. Large yellow circles indicate >2 strong positive signatures for microbial life were detected at the locale, while small yellow circles suggest at least 1 strong positive signature (see Table 3). Images to right provide examples of the habitat types encountered along the traverse: a) locale 1, cloud cover or fog in distance; b) locale 1, RGB image of lichens on exposed soil crust; c) locale 1, chlorophyll FI image of lichens; d) locale 5, promising rock habitat for endolithic-type microorganisms; e) locale 5, habitat in (d) with grey rock; f) locale 5, chlorophyll FI image, note horizontal band in left image typical of endolithic or chasmolithic communities; g) typical microhabitat at locale 7; h) locale 8, hill with white rocks (good habitat for hypolithic microorganisms), drainage channel and exposed layered outcrops in background, note plant in channel; i) close-up of white rock habitat in (h); j) soil/rock habitats in locale 19; k) locale 19, same area as in workspace image in (j) showing lichens; l) locale 19, chlorophyll FI of lichens in (k). Stereo Panoramic Imager, SPI = 21.9° × 15.9° field-of-view; Workspace camera, WI = 1.5 m × 1.3 m; Fluorescence/Microscopic Imager, FI = 10 cm × 10 cm.

detecting microorganisms. Second, because many terrestrial hyperarid deserts often contain sparse and/or widely dispersed microbial life, an engineering and science goal of the field experiment was to ensure that relatively great distances were covered each sol. By exploring great distances, random sampling would thus allow, in theory, a larger area and greater diversity of habitats as well as a higher number of microbial samples to be collected.

[19] During ground-based mapping and exploration, the remote science team generated and transmitted to the rover a daily plan that instructed the rover to (1) traverse specific distance(s), so that targeted regions of interest could be reached and studied; (2) carry out specific activities, such as spectroscopy for mineralogy; and (3) acquire a minimum number of samples, particularly with the goal of detecting life with the FI instrument.

3. Results

3.1. Selection of Orbital Regions of Interest, Site B Example

[20] Prior to the rover traverse, multiple regions of interest were identified within Site B based on the process and biological selection criteria described above. Major water-associated features (e.g., drainages and drainage basins, distinct alluvial fans, evaporites such as carbonates) identified as potential targets of biological promise included

the large south-central basin (Figure 2) and an area designated 'trap door southwest' (Figure 2) located east of a main gap in the coastal range. Other areas where fog might accumulate (e.g., west-facing promontories) or funnel (e.g., gaps in coastal range, Figures 2 and 3) also represented high priority regions based on the 'follow the water' strategy. VNIR orbital imagery detected signatures for chlorophyll and/or evaporite minerals (1) on the western and eastern faces of the coastal (Pacific coast visible in orbital imagery) mountains (m), and (2) in the northwestern region near the geologic contact that separates unit f from unit m (Figure 3). Other features of astrobiological interest included possible desert pavement landscapes in unit f and d1 (on the slopes of alluvial fans) and hypersaline environments at topographic lows and terminus of drainage channels at the south-central basin. Regions where multiple criteria converged became the highest priority, including: 1) the dense chlorophyll region near eastern face of the coastal range (Figure 2), (2) drainage/ponding areas in the south-central basin (not reached), and (3) the confluence of major drainage systems at the contact between alluvial fan (unit f) and dissected (unit d1) materials. It should be noted that, while initial selection of regions of interest was based on the above criteria, these decisions did not preclude the search for unique or unexpected habitats or microbial life during the rover field experiment.

3.2. Ground-Based Traverse Results: Site B

[21] During the 6-km Site B traverse 13 locales (Figure 3) were mapped and sampled. Tables 3 and 4 contain ecology, mineralogy, geology and microbiology data for each locale. Below, we present a synthesis of important findings or implications, rather than a comprehensive, in-depth traverse review.

[22] Overall results from Site B habitat mapping are presented pictorially in Figure 3, which highlights the importance of scale in habitat mapping and the search for life. From a geological perspective, during the 6-km traverse the rover surveyed dissected plains-forming materials (unit d1, interpreted to be lacustrine, alluvial, and fluvial deposits), a major drainage unit (catchment site for units m, f, and d1 materials), and a unit (f) comprised of multiple alluvial fans of varying relative age and albedo [*Dohm et al.*, 2005]. In contrast to geological diversity, however, if the 6-km traverse is analyzed strictly from ground-based habitat and mineralogical perspectives, Site B is predominantly a homogenous desert pavement environment. Thus, from these latter two perspectives, the broadest interpretation of the entire traverse results is that, despite the distance covered, only one main habitat type—desert pavement—and one main mineralogical type—clays (soil surfaces)—was encountered. This result is, in part, a reflection of the random and limited targeting and sensitivity of the VNIR instrument to particular compositions, and/or the presence of rock dust coatings that spectrally resemble clays.

[23] Microscale analyses from the workspace and FI data reveal, as expected, greater diversity, which was reflected by variations in soil surface composition, rock size and density, and morphological and textural differences. Indeed, at the microscale, each locale and FI sample itself can be considered a universe of individual microhabitats (m to nm scale), which reflects heterogeneities in climate, geology and mineralogy. Distinct microhabitat types surveyed at Site B included (Figure 3): (1) various clay minerals, sulfates and unaltered parent rock comprising desert pavement, (2) dark volcanic rocks; and (3) translucent rocks and salts (sulfates, including gypsum). Incorporation of the FI data into larger-scale analyses enabled macroscale habitat classifications of the traverse that, in fact, better reflected the diversity predicted from orbital geological interpretations. Thus, by integrating multi-scale data sets, the Site B traverse could ultimately be characterized as containing 5 main habitat zones, or units (Figure 3):

[24] 1. Desert pavement habitat unit (locales 1–4): comprised of exposed clay surface crust (possible lacustrine origin) covered by low density of mostly small pebbles ($\sim\leq$2 cm) of varying composition within geological unit d1.

[25] 2. Drainage habitat unit (locale 5): geologic contact separating geologic units d1 and f; poorly sorted, angular to subangular rocks (interpreted as mostly igneous and sedimentary origin); the unit contained a diversity of boulder and rock habitats, including those typically colonized by lithophytic microbial communities.

[26] 3. Transition zone (locales 6–7): alluvial fan materials of geologic unit f containing habitats that were similar to (from SPI and microscopic images) those in the desert pavement habitat unit above but with rock composition and density (at the mm and cm scale) more characteristic of those in locales 10–19 (Figure 3).

[27] 4. Drainage channel unit (locale 8): alluvial fan with major drainage that exposes rock outcrops, which includes layered deposits; various types of promising rock habitats and possible salt deposits.

[28] 5. Alluvial fan unit f (locales 10–19): typical alluvial fan landscapes; hillslopes carved by drainage channels with alluvial/fluvial deposits and terraces overlain with pavement of high pebble density but varying composition, including translucent (granites, quartz, salts) and volcanic rocks (from visual evidence). Immediately ($\sim$few mm) below the surface pavement, a soft salt (spectroscopy indicated minor gypsum at 8 and 14, barite at 11) soil layer was observed.

[29] During the traverse, positive signatures for microbial and plant life were detected, to a varying degree of certainty, at 9 of the 13 locales (Table 4). Locale 19 was particularly important, since dense lichen populations were detected (FI (visible), via color and textural clues), and positive chlorophyll, DNA and protein FI signatures were acquired. Weak to strong positive chlorophyll signatures, which were overwhelmingly associated with visible (FI RGB) surface lichens, were detected at 62% of all locales (Table 4). Although especially abundant at locale 19, sparse lichens were also detected visually and with fluorescence (Weinstein et al., submitted manuscript, 2007) on raised surface crust microhabitats at locales 1 and 2. Photosynthetic and non-photosynthetic lithophytic bacteria and/or lichens surviving in the exposed cracks of rock microhabitats at Locale 5 were also detected remotely.

[30] Overall, positive DNA and protein FI signatures acquired during the traverse suggest the presence of bacteria at most of the locales in Site B. Similarly, post-project data released to the science team showed that complementary laboratory studies of heterotrophic bacteria from soil samples at Site B locales indicated abundance ranging from <1

Table 3. Landscape-Scale (m to km) Habitat Assessments and Results for Site B (From Orbit, SPI and Ground-Based Spectroscopy)

Geologic Unit/Orbital Region[a]	Locale	Major Landscape/Habitat 'Type'[a]	Distinguishing Features	Mineralogy[b]	Past/Present Water Activity?[c]	Priority in Terms of Potential for Life[d]
unit d1	1	possible lacustrine, fluvial, and alluvial deposits; DP/crust, tiny pebbles; aeolian mantle	polygons, surface crust, heaves; fractures, few rocks	clays, sulfates, IO, AV	fog/low clouds near coastal range; PAA (DC)	low (orbital and SPI)
unit d1	2	similar to locale 1, but more rocky with small pebbles	similar to locale 1	clays, sulfates (alunite, anhydrite), AUV, IO	similar to locale 1	low priority (orbital and SPI)
unit d1	3	similar to locales 1–2; finer soils, some large rocks, pebbles	visible drainage channels in pan	clays, AUV, IO	similar to locales 1 and 2	low priority (SPI)
unit d1	4	similar to 1–3, higher density of rocks	lighter surface crust, exposed crust and tiny pebbles	clays, AV, IO	no SPI	low (SPI & FI)
major drainage, geologic contact of units d1 and f	5	DP, AF with drainage channels, drainage channel with abundant rocks/boulders	Larger rocks, possibly igneous (granites, translucent rocks	clays, AV	similar to locale 3; PAA (major DC for units d1, f, m)	high (good habitats for L and lichens, (orbital, SPI & FI)
unit f	6	DP, AF materials, very fine soil and some pebbles; resembles 4 from pan	white pebbles (salt? quartz?); high pebble density & different compositions (from FI)	clays and IO	some clouds/fog W/SW of range, PAA (AF)	moderate L, H (SPI)
unit f	7	DP, large and high rock density (coated with dust/varnish)	exposed white outcrop, white rocks (quartz?) in FI	no data	similar to 6	low, L (FI)
unit f (drainage channel near range)	8	DP, AF materials, small hills & slopes, major drainage channel, with exposed outcrops	White stones (quartz, salt ?; spectra later confirms gypsum), exposed outcrops (white)	sulfates (gypsum), clays, AUV	similar to 6–7; distinct drainage channels in SPI	high, L (orbital & SPI), low priority (FI)
unit f	10	DP—larger/angular rocks, rocks with dust/aeolian material	Dark, embedded rocks; runoff channels, high rock density	clays, AUV	a few clouds behind range	moderate, L (SPI), low from FI
unit f	11	similar to 10	Surface seems harder/more consolidated than locales 7–8	clays, IO, sulfates (barite), AUV	similar to 10	(same as locale 10)
unit f	14	similar to 10–11	deep, incised channels	sulfates (gypsum), clays, AUV, IO	clouds/fog close behind slope	same as locale 10–11
unit f (chlorophyll area in IKONOS)	19/20	large sloped runoff channels; good habitat for lithophytes	large rocks & boulders—color, appearance and distribution indicate possible eroded quartz or other friable rock or salt.	clays, sulfates (alunite) AUV, IO	high impact from fog predicted & confirmed (SPI, rover energy data)	high, (chlorophyll & high water influence, good habitat for L (orbital, SPI, FI)
unit f	24	gentle sloped runoff channels, fan terrace; extremely rocky	same as locale 19, good habitat for L (translucent rocks in SPI)	no data	heavy fog (SPI)	no data

[a]Initial interpretations catalogued during remote field operations. Geologic units, d = dissected, plains-forming materials, f = alluvial fan materials. Other abbreviations: DP = desert pavement, which refers to alluvial fan materials/gravels that mantle surface soils; FI = fluorescence RGB image; SPI = panoramic camera image; L = lithophytic organisms (including endoliths, chasmoliths, hypoliths, etc.); H = halophilic organisms.
[b]Results from ground-based spectroscopy, with all samples from surface rocks and soils, IO = iron oxides, AV = altered volcanics; AUV = altered/unaltered volcanics. See *Piatek et al.* [2005] for details.
[c]Presence of fog or clouds in rover panoramic image and/or past aqueous activity (PAA) based on geomorphologic signatures such as visible drainage channels (DC) and alluvial fans deposits (AF).
[d]Potential for life from orbital and SPI data, unless otherwise specifically noted.

Table 4. Microscale (cm) Habitat Assessments From Workspace (WI) and Microscopic/Fluorescence (MI/FI) Images for Individual Locales Sampled by the Rover Within Site B

Locale	Microhabitat Features From FI	Distinguishing Features	FI Results[a,b,c]
1	exposed crust, small pebbles (various compositions based on color)	cracks/crevices of exposed crust; orange tint (Fe from spectra) to crust; some pebbles w/varnish	**V**, **C**, **D**, P lichens on surface crust
2	similar to locale 1 but darker, higher rock density	many dark, reddish-orange rocks, mineral coating/desert varnish (orange/red) on rocks	**V**, **C**, D, P Orange lichen
3	similar to locale 1–2	pebble in crack of surface crust-positive chlorophyll; orange pebbles that could be mistaken for lichens found at locale 2	V, **C**, *D*, *P*
4	similar to 1–3		V, C
5	very different- many small rocks, possible translucent and granitic rocks	horizontal 'grey' band on rock that has positive chlorphyll signal; good lithophyte habitat	V, **C**, *D*
6	mostly surface crust with small rocks, similar to locales 1–4; higher rock density and composition like 7–19	translucent and igneous rocks (granitic appearing from color, good for lithophytes), cracks/polygons in crust; edge of red rock grey spots positive in chlorophyll	V, **C**, *D*, P
7	highest pebble density. Composition similar to 6 but greater abundance darker materials	translucent rocks (quartz? salt? other)	*V*, *C*, *D*, *P*
8	mostly small pebbles, few white rocks, more igneous-type materials, similar to 6–7	chlorophyll signature in small depression in image, surface crust showing as in 1–4 and 6	*V*, *C*, D, P
10	high pebble density, lighter materials than locale 7	some translucent and grey/dark pebbles (appeared volcanic; sedimentary not ruled out)	*V*, *C*, D, P
11	desert pavement overlaying crust. mixed compositions, similar to 10	grey spot on rock (possible lichen?)	*V*, **C**, D
14	similar to 10–11.		*V*, *C*, **D**, **P**
19	similar to locales 6 & 8, lower pebble density/more exposed crust other MI like locales 7–14, high pebble density	post-plow images reveal near-surface layer (soil texture soft and granular) with white pieces, (embedded in crust prior to plow maneuver)	Multiple FI samples acquired. Lichens. **V**, **C**, **D**, **P**
24	same as 19	crust material, cracked; mostly exposed but also tiny pebbles (orange/black, igneous-looking).	*V*, *C*, D, **P**

[a]Symbols are bold if dye signal was positive for any sample at a locale (rating of 2); symbol with no bold or italics indicate a weak positive signal (rating of 1) or ambiguity in the data; italics indicate no positive signal (zero rating); if no data were available for a particular dye, then the symbol is not shown.
[b]For detailed FI results, see *Weinstein et al.* [2005]; protein application did not work until locale 5; WI images not available until after locale 8.
[c]Abbreviations: V = visual (morphology, texture), C = chlorophyll, D = DNA, P = protein.

to 1×10^4 colony-forming units/g-soil (CFU/g-soil, determined as MPN enumerations on 1/10 strength PCA medium). The geometric mean of 38 samples from the 10 locales was 32 CFU/g-soil. Surprisingly, however, most locales at Site B exhibited low soil heterotrophic abundance at <1–10 CFU/g-soil, which may reflect the site's low mean annual rainfall (<5 mm). Highest abundance, supporting the orbital predictions of a promising biological region, occurred at locale 5 (1×10^4 CFU/g-soil) and locale 8 (1×10^2–10^3 CFU/g-soil), but also at locales 1–2 and 7 (not predicted from orbit). Patchiness in microbial abundance was observed in the culturing studies for most locales, for example from <1 to 1×10^3 CFU/g-soil at locales 1–2, and this spatial heterogeneity in microbial distributions has been noted elsewhere for hyperarid soils in the Atacama Desert [*Navarro-González et al.*, 2003; *Lester et al.*, 2007].

[31] Ground-truth by the remote science team at Site B in Jan. 2006 allowed interpretation of earlier conclusions reached from remote data on the abundance and diversity of microbial life at several of the Site B locales. In general, remote rover-based assessments significantly underestimated both the diversity and abundance (as compared to in-situ visual inspection in the field) of microbial communities at the locales. At locales 1–5, for example, lichen abundance was roughly 80% higher than that estimated during FI-based remote operations, and locale 8 contained cyanobacterial soil crusts and abundant lichens, neither of which were identified during remote operations. There may be several reasons for this. First, and most significantly, was the limited number of samples taken per locale, which was an outcome of technical rover operation constraints (e.g., 1 hour for each FI sample). Second, dye penetration issues (a result of extremophile microorganisms' tough external cell walls/glycocalyx), reduced the effectiveness of fluorescent dyes [*Weinstein et al.*, 2005]. Third, many microbial communities were located in hard-to-reach areas (e.g., steep drainage channels) or in habitats that instruments were incapable of sampling (within rocks and/or sheer faces of terraces). Fourth, temporal variations in moisture (e.g., fog intensity) might explain (at least in part) the observed differences in lichen abundance, which were also noted by the robotics field team for 2004 versus 2006.

[32] Meteorological data (at locale 1) and SPI imagery provided further contextual understanding (albeit short-term) of habitat climate and microbiology in Site B. Fog and low-lying clouds were confirmed in SPI images and by on-board rover sensor data, which showed a diurnal relative humidity pattern for locale 1 typical of night-time marine fog incursion (with $\geq$95% relative humidity reached) and its dissipation after sunrise. Wind speed and direction shifts, along with breaks in rover solar insolation data, likewise showed signs (e.g., breaks in solar insolation) typical of fog

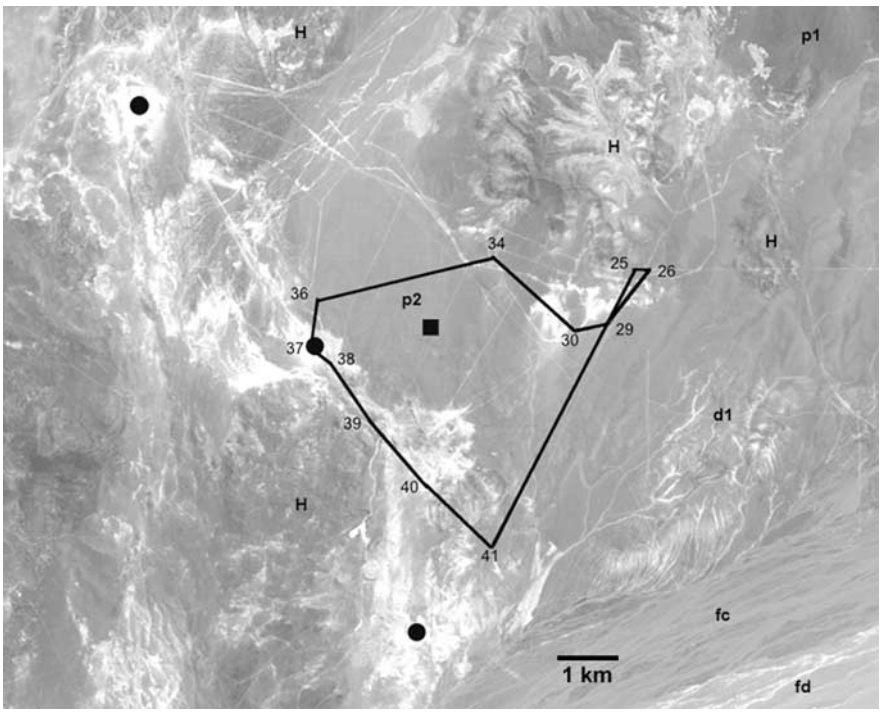

Figure 4. Schematic map of Site C showing pre-traverse, satellite-based reconnaissance and ultimate rover path. Geologic map units include: H – hilly materials; p1 and p2 – dark and moderately dark plains-forming materials, respectively; d1 – dissected materials; fc, and fd – flow materials. Black dots mark interpreted paleohydrologic activity and black square indicates spectroscopic signatures consistent with quartz.

and further supported the marine fog incursion hypothesis. It became evident by sol 6 that the general region encompassing all Site B locales, extending from the western coastal range inland to locale 1 (~4 km from coast), receives significant fog. Indeed, fog constrained rover operations during sol 6, and altogether prevented them during sol 7. The availability of fog at Site B explains the presence of abundant lichen populations, which utilize atmospheric water vapor, at several locales.

[33] Several important insights can be concluded from Site B regional mapping and ground-based life detection results. One is the success of predicting favorable habitats for life from orbital and landscape (e.g., panorama) data. For locale 5, several disciplinary lines of evidence converged to predict this region as a priority for biology, suggesting it would be a primary drainage with streamlined bedforms and a routing/ponding site (for unit d1, m, and f materials, see Figure 2) that would contain an aqueous-impacted area with a diversity of rock types and sizes (i.e., promising habitats for lichens and lithophytic microbes). These predictions were confirmed by ground-based SPI images; by spectral data, which showed weathered materials; and by FI data, which detected chlorophyll signatures on rocks. Together, each of the independent lines of evidence (orbital and ground scales) predicted and confirmed a promising locale for microbial life. Another example was locale 19, where follow-the-water and satellite spectra predictions accurately guided the rover to an area abundant with microbial life. This locale is situated near the high priority region of interest (see section 3.1) that had strong chlorophyll signatures and visible influence by marine fog (later confirmed at the locale by SPI and climate sensor data). These successes reiterate the importance of climate sensors and real-time analyses and mapping of past and present water activity at multiple scales (from orbit to the microhabitat).

[34] Nevertheless, despite the above successes, experiences from other Site B locales demonstrate that orbital predictions are insufficient alone to identify many promising habitats. As one example, orbital, mineralogical, and geological interpretations and rover-acquired SPI data did not initially identify geologic unit d1 (Figure 3) as a priority region for microbial life. Yet, all locales in this (1–4) unit contained abundant lichens (and other communities), as partly shown during remote operations but more strongly confirmed during ground-truth.

3.3. Site C Results

[35] While ASTER VNIR imagery showed no significant chlorophyll signatures at the orbital scale, several regions of interest (Figure 4) were identified prior to the traverse at Site C, the 'dry' site:

[36] 1. A region of potentially high concentrations of quartz (good biological habitat for photosynthetic microbes), as indicated from the TIR mineralogy map, within the plains-forming materials (geological unit p2, Figure 4).

[37] 2. Regions where past or present aqueous-associated activity was evident—follow the water strategy—such as

the regions with high albedo in the ASTER image (e.g., small topographic basins as possibly hypersaline) and TIR mineralogy map signatures suggesting the presence of evaporite minerals. These regions occur at several places within the dissected plains-forming materials (geologic map unit d2, Figure 4).

[38] During a 24-km science traverse, 10 locales were mapped (Tables 5 and 6). Macroscale habitats encountered at Site C but not at Site B included hypersaline and quartz-rich environments. Subsurface soil habitats were also accessed at Site C by a plow mounted below the rover that removed ~1 cm of surface soils (Figure 5).

[39] As at Site B, pre-traverse orbital analyses were highly successful in identifying promising regions of astrobiological interest and macroscale habitats in Site C. These predictions, particularly from TIR mineralogy maps and follow-the-water strategies, meshed well with ground-based microhabitat FI data. From orbital and ground-based results Site C can be broadly divided into two major habitat units:

[40] 1. Desert pavement unit: locales 25–34 (geological units d1 and p2, Figure 4); TIR mineralogy and MI ground-based data confirm varying rock densities, sizes and compositions; unit consists of surface pavement overlaying near-surface soils comprised of salts (mainly sulfates); interpretations during remote operations included evaporitic materials (e.g., gypsum) or alteration minerals such as talc/clays for white materials and iron oxides for darker materials. Some locales (25, 34) also contained a relatively high abundance of quartz.

[41] 2. Hypersaline unit: locales 36–41 (geological unit d2, Figure 4) occurred in the drainage/catchment area, which included rock materials such as ash flow and evaporite deposits.

[42] Within the two broad units, finer-scale habitat diversity distinctions were observed. Locale 25 contained rocks (amorphous quartz) within a darker rock pavement (also locales 26–30), as well as exposed white materials, which were interpreted to be sulfates (Figure 5). Traversing across the p2 geologic unit (Figure 4), higher quartz rock abundance was predicted and observed at locale 34. Spectral data indicated minor ($\leq$25% of observed surface) amounts of sulfates (alunite and gypsum) at locales 25 and 34, and MI data of plowed samples revealed a soft near-surface soil layer (Figure 5), which was confirmed at locale 38 to be gypsum. This near-surface sulfate layer has been observed throughout the Atacama Desert, particularly in its driest regions [*Ericksen*, 1983; *Rech et al.*, 2003; *Ewing et al.*, 2006]. As the rover entered unit d2 at locales 36 and 38, desert pavement gave way to materials comprised of both volcanic (ash flow deposits) and evaporite/salt-type environments (locales 36–41, Figure 5). This transition to increased aqueous-associated habitats was predicted from orbital TIR and VNIR data. Ground-based spectra showed minor sulfates at locales 36–38. However, at locale 36 MI data also revealed a unique-looking microhabitat confirmed by spectroscopy to be volcanic ash. Fine-scale (MI) habitat distinctions could also be seen for locales 39 and 40, which contained more dark albedo (altered volcanics) rocks than locales 38–41—a ground-based MI result predicted from orbital TIR spectra.

[43] Positive signatures for microbial life were detected at all 8 locales in Site C where FI data was acquired (Table 6), including on dark and light albedo rocks. Positive chlorophyll signatures were observed at only 37% of locales sampled by the rover—a much lower percentage than at Site B—and this trend is explained by the absence (based on FI RGB visual evidence) of surface lichen populations at Site C. Possible endolithic bacteria were imaged at locales 25, 34 and 38, with thin bands visible in rocks in the MI and correlated with FI chlorophyll, DNA and/or protein signals. (The presence of chasmolithic cyanobacteria in quartz rocks at locale 25 was confirmed during ground-truth). Other soil bacteria may have been associated with the strong fluorescence signals in samples from locale 36, as well associated with white materials at many other locales (e.g., 25, 26, 34).

[44] Based on remote analysis of rover-acquired FI data, Site C had lower overall biological diversity than Site B, with no visible (SPI or FI) or fluorescence (chlorophyll) evidence for the presence of plants or surface life such as eukaryotic lichens. In contrast, the abundance of non-photosynthetic microbes (as indicated by positive fluorescence in DNA and protein channels) appeared to be similar relative to Site B. This was surprising, but may be explained by the similar mean annual rainfall of the two sites (~5 mm)—which dictates soil bacterial abundance—but more frequent fog—which influences surface lichen abundance—at Site B. Meteorological data (locale 25) collected during remote science operations indicated Site C was much drier than Site B, with a minimum air relative humidity of $\leq$5% (versus ~60% at Site B) and maximum of 25% (versus $\geq$95% at Site B, associated with fog). SPI imagery and solar insolation data also suggested a relatively cloud-free environment, and no evidence for fog was obtained from climate or SPI data, which likely explains the absence of surface lichens.

[45] Ground-truth surveys (Jan. 2006) supported conclusions by the remote science team that Site C had a relatively harsher climate and less diverse biological surface life than Site B. Laboratory studies likewise found very low bacterial (heterotrophic) numbers, ranging from <1 to 10 CFU/g-soil, at all Site C locales other than locale 36, which had the highest MPN (1×10^2 CFU/g-soil). These comparably low numbers between many locales at Sites B and C mirror the findings from the rover-acquired FI (DNA and protein signatures) data showing similar relative abundance, and are in line with previous work on the hyperarid soils of the Atacama [*Navarro-González et al.*, 2003; *Lester et al.*, 2007]. In contrast, however, Site C locales overall exhibited a geometric mean of 3.2 CFU/g-soil—a nearly ten-fold decrease in overall abundance from Site B. Also in contrast to Site B, in general more positive signatures were detected remotely by fluorescence during rover operations at Site C than observed by field scientists visually during in-situ ground-truth inspections. Finally, the significance of certain habitats encountered during the Site C traverse was underestimated. Quartz rock abundance at locale 25, in fact, was significantly higher than at locale 34, making it an ideal area to search for photosynthetic organisms. Spectral data (post-

Table 5. Landscape-Scale (m to km) Habitat Results for Site C (From Orbit, SPI and Ground-Based Spectroscopy)[a]

Geological Unit/Orbital Region	Locale	Major Landscape/Habitat Type	Distinguishing Features	Mineralogy	Past or Present Water Activity?	Priority in Terms of Potential for Life
unit d1, dissected terrain	25	DP, high rock density translucent materials later confirmed by spectra as salts; some large (~m), dark rocks	white rocks (SPI, WI); Post-plow soil layer texture soft & granular), white pieces	clays, sulfates, AUV, (alunite), IO, quartz (soils and rocks)	clear skies, PPA (DC; polygons in pan)	extremely high (SPI, WI, FI)
unit d1	26	DP, many large rocks, more large dark rocks and surface crust; grey coating/varnish on rocks	possible ponding in topographic low (from SPI)	clays, sulfates (alunite), AV	similar to locale 25	low (SPI, FI)
unit d1, white patch in ASTER	29	similar to locale 26, DP, fewer large rocks/boulders than 26	(similar to locale 26 but exposed lighter surface, also similar to 30 in SPI and WI)	clays, sulfates (alunite), AV	similar to locale 25	high (orbital) low (SPI, FI)
unit d1, dark area in ASTER	30	similar to 26–29, but few large rocks; polygons on surface soils	grey tone/coating on rocks	clays, sulfates (barite, alunite), quartz, AV, IO (soils and rocks)	similar to locale 25	low
unit p2, pronounced quartz area (TIR map)	34	DP, Unique locale for quartz rocks large rocks in SPI; dark and light/white rocks in WI, varying sizes	gypsum, quartz; desert varnish on rock?; Post-plow as at locale 25	clays, AV, sulfates (gypsum, barite, alunite), quartz, IO (soils, rocks, plow)	high light clouds possible paleofloodplain (fluvial deposition)	extremely high (orbital, SPI, FI)
unit d2 high albedo area	36	different-looking habitat vs. previous locales; white rocks; uniform soil/salt igneous? crust (can see rover tracks)	exposed white patches (SPI); VERY unique looking surface composition/texture (MI)	clays, sulfates, AV (alunite), quartz, IO	high clouds, PAA (paleo- DC, ponding; polygons in panorama)	high (orbital, FI)
unit d2 high albedo area	38	unique and extensive evaporite/salt habitat; felsic rocks (interpreted to be ignimbrites or rhyolites); few to no large rocks	interpreted evaporite or igneous rock materials (SPI); different from previous locales	sulfates (gypsum, alunite), clays, quartz, AV, IO (soils and post-plow)	similar to locale 36	very high (orbital, SPI, FI, H habitat)
unit d2 high albedo area, contact unit	39	small/tiny dark pebbles overlying greyish-white, highly cemented surface crust	no SPI pan here	no data	similar to locale 36	low priority (SPI)
unit d2 high albedo area	40	unique-looking locale terraces covered by small dark stones embedded in tan, highly cemented crust	dark pebbles with white inclusions (see spectral results); incised gullies at terminus of hills/terraces; exposed outcrops	clays, sulfates (gypsum, alunite), AV, quartz (soils and rocks)	similar to locale 36	low to mod. (SPI)
unit d2 high albedo area	41	DP; large areas of white exposed materials; large dark rocks (low density); looks similar to locale 25	interpreted evaporite and igneous rock materials; possible playa in foreground; mix of DP & hypersaline habitats	AV, quartz	similar to locale 36	high (SPI)

[a]See Table 3 for abbreviations. All spectroscopy samples were of surface soils (top 1 cm), unless otherwise noted.

Table 6. Microscale Results From Workspace and Fluorescence Imagers for Individual Locales Sampled by the Rover at Site C

Locale	Microhabitats	Distinguishing Features	FI Results[a,b]
25	high density of pebbles, mixed compositions (dark red & black, small white pebbles	positive signatures in cracks of rocks, grey lines in small black pebble	*V*, *C*, **D**, **P**
26	similar to locale 25, lower pebble density, more exposed surface crust	white, red and dark pebbles	*V*, *C*, **D, P** esp. in white materials
29	similar to locale 26, more exposed surface crust exposed	positive signatures especially on light-colored surface crust/soil and rocks;	*V*, *C*, **D, P** protein uniform on rocks
30	different from 25–29, more white rocks, other compositions	white rocks that look like quartz, igneous materials such as ignimbrites, or salts, with some varnish	*V*, *C*, D, **P**
34	similar to 25–30, little exposed crust, highest density white rocks, which confirmed by spectra to be quartz (MI)	clear post-plow 'puffy gypsum' (spectra confirmed) soil layer; white pieces of gypsum/salt (texture) in post-plow MI image	*V*, **C**, **D**, **P** Strong horizontal band on red rock
36	completely different than previous locales; few to no pebbles	"loofa"-like pieces of salt materials and exposed surface crust; Almost every structure on these materials had positive signatures	*V*, **C**, **D**, **P**
38	dark surface and pavement (WI vs. SPI); grey exposed surface crust	small salt pieces, puffy gypsum appearance after plow, very uniform few to no pebbles.	*V*, C, **D**, **P** horizontal line for C
39	no data	no data	no data
40	very different surface than previous locales; few, angular dark pebbles embedded in greyish-white crust	looks more like volcanic influenced area (dark pebbles mantling surface crust)	*V*, *C*, **D**, **P**
41	no data	no data	no data

[a]Symbols are bold if any dye signal for any sample at a locale was positive (rating of 2); symbol with no bold or italics indicate a weak positive signal (rating of 1) or ambiguity in the data; italics indicate no positive signal (zero rating); if no data were available for a particular dye, then the symbol is not shown.
[b]Abbreviations: V = visual (morphology, texture), C = chlorophyll, D = DNA, P = protein.

operations) at locale 25 also revealed barite and hectorite—a mineral often associated with past thermal spring activity. And at locale 36, the significance of a large ash deposit—from which laboratory cultures showed the highest heterotrophic bacteria abundance in Site C—was overlooked during remote operations.

[46] Because Site C was the more "extreme" (i.e., drier) environment, additional laboratory studies were carried out to assess bacterial soil diversity (aerobic heterotrophs) by phylogenetic analyses, which revealed a total of 31 bacterial species at the Site C locales representing 4 phyla and 14 genera (Table 7). Seventy-five percent of the locales contained two or more species, two locales contained only one species, and one (locale 30) contained no culturable heterotrophs (at a detection level of 1 CFU/g-soil). Only four phyla were represented: *Actinobacteria* (22 strains, all in the order *Actinomycetales*), *Proteobacteria* (5 strains), *Firmicutes* (3 strains) and *Bacteriodetes* (1 strain). *Arthrobacter* species were the most common genus, followed by *Kocuria*. These results are comparable to those from the few previous studies of microflora in the soils of the driest portions of the Atacama Desert [*Navarro-González et al.*, 2003; *Drees et al.*, 2006; *Lester et al.*, 2007] The preponderance of *Arthrobacter* species (and its close relatives) is not surprising, given their desiccation resistance and ability to survive low nutrient levels. Two locales (25 and 38) contained strains that grew in the presence of 2 M NaCl (Table 7). The above results suggest that Site C habitats contain diverse microbial communities even within the small 10-cm^2 areas sampled by the rover at each locale.

4. Lessons Learned

[47] Pre-traverse, satellite-based analyses were a critical part of the LITA 2004 success in accurately identifying many (but not all) promising macroscale habitats in the Atacama Desert, and in predicting not only key habitat transitions but also microscale geological and habitat diversity. The findings demonstrate the efficacy of an orbital-to-ground, follow-the-water approach, in which smart orbital reconnaissance and traverse planning pinpoint and target promising biological "hot spots," especially those associated with past or present aqueous activity. However, it should be noted that not all life-containing habitats—some of which had high abundance of surface life—at Sites B and C were targeted or discovered via the follow-the-water approach.

[48] The LITA field experiment also confirmed the critical need for astrobiology missions to tightly integrate disparate scientific disciplines. Science team geologists and mineralogists not only carried out orbital, regional

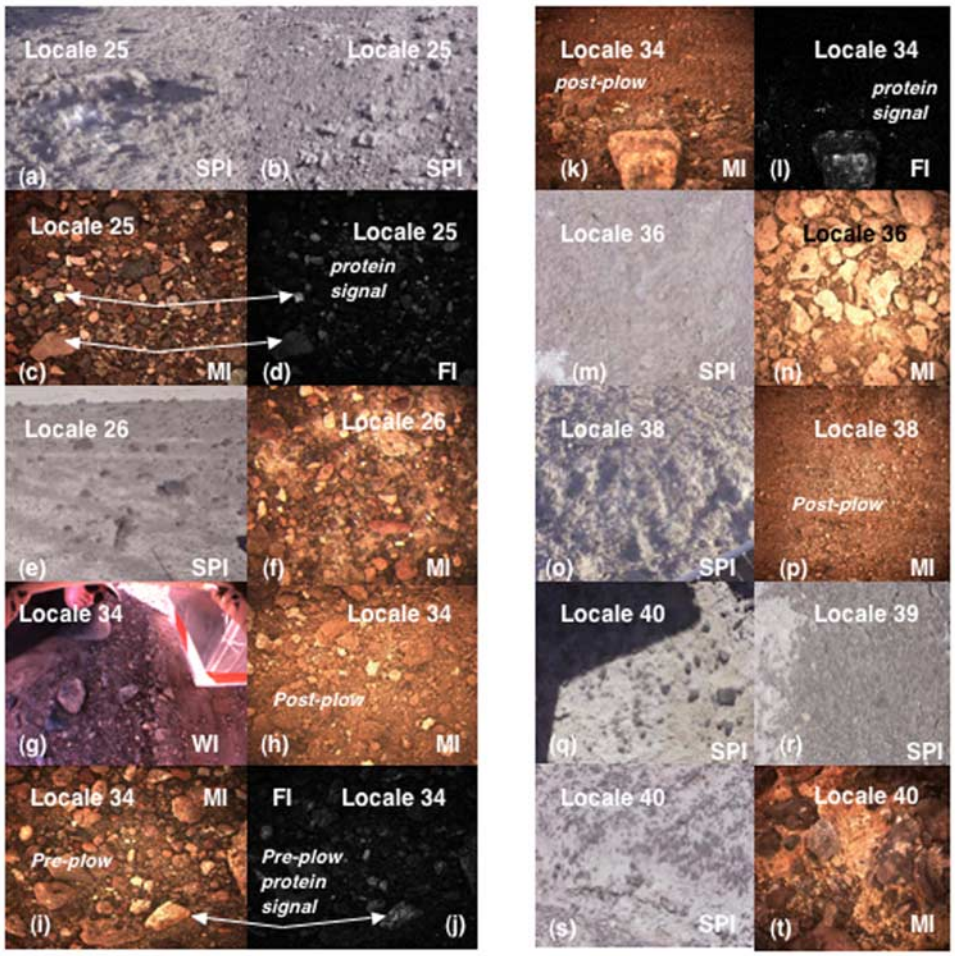

Figure 5. Site C rover-acquired habitat images: (a) gypsum evaporite deposits; (b) amorphous quartz; (c) pebbles of varying color and size; (d) DNA fluorescence signal on pebbles in (c); (e) dark desert pavement with large rocks; (f) pebbles and exposed crust; (g) workspace image with plowed area in right part of image; (h) microscopic image (MI) of plowed area showing subsurface ($\sim$1 cm) soil layer with white pieces of gypsum; (i) pre-plow pebbles; (j) pre-plow positive protein signatures; (k) post-plow image, showing white rock (gypsum or quartz, not confirmed); (l) positive protein signature of rock in (k); (m) contrasting (with n) habitat SPI perspective; (n) porous material (ash deposit) in (m); (o) salt-flat type appearance of habitat from SPI image (p) similar type of near-surface gypsum soil layer as in (h); (q) volcanic rocks embedded in soil surface; (r) dark desert pavement at locales 39 and (s) locale 40; (t) MI view of (s) provides clearer perspective on dark pavement habitat. Scales: SPI = 21.9° $\times$ 15.9° field-of-view; WI = 1.5 m $\times$ 1.3 m; MI = 10 cm $\times$ 10 cm.

and landscape interpretations, but also actively worked with microbiologists to conduct daily microhabitat surveys—providing *real-time* mineralogical and geochemical context. The importance of this close cooperation is evident in that the first positive discovery of microbial life during the field experiment was made by a geologist.

[49] The tight integration of disciplines during the LITA field experiment also raised another important issue—one of *scale*. The rover instruments and team's ability to shift seamlessly from orbital to regional to microscale data collection and analysis—and back again—was fundamental to the remote detection and study of habitats and life in the Atacama. Varying (and often subconscious) perceptions of scale influence engineering and science decisions alike, including the type and locations of rover instruments, sampling frequency, and the time/bandwidth allocated to competing sampling and mapping demands. A microscale (mm to nm) focus should explicitly permeate all aspects of a robotic mission that searches for life beyond Earth, from management to engineering to science, and rover on-board instrumentation should co-locate biological, mineralogical, geological and climate data at the microbial and all larger contextual scales.

[50] **Acknowledgments.** The authors thank the LITA rover engineering team for their unstinting efforts in the field. We also acknowledge invaluable translation and communication assistance by the project's IT Eventscope team. K. Rhodes and two anonymous reviewers improved the scope and clarity of the manuscript, and their constructive comments are

Table 7. Aerobic Heterotrophic Bacterial Species Isolated at Site C Locales

Locale	Genera Identified[a]
Landing Site	*Arthrobacter* (pink)
25	*Kocuria*[b], *Arthrobacter* (white)[c], *Kytococcus*[d]
26	*Arthrobacter* (white), *Burkholderia*, *Arthrobacter* (pink), *Bacillus*, *Oxalobacteraceae* family
27	*Paracoccus*
29	*Kocuria*, *Bacillus*
30	
34	*Arthrobacter* (pink) (2 varieties), *Arthrobacter* (white), *Kocuria*
34b	*Arthrobacter* (pink), *Blastococcus*, *Arthrobacter* (white)
36	*Kocuria*, *Arthrobacter* (pink), *Arthrobacter* (white), *Brevundimonas*
38	*Planomicrobium*[b], *Arthrobacter* (pink)[c], *Arthrobacter* (white)[c], *Arthrobacter* (white)[d]
40	*Micrococcus*, *Pseudomonas*
25 (runout)	*Janibacter*, *Chryseobacteium*

[a]Strains are listed in their approximate order of abundance based on the MPN dilution from which they were isolated, and their relative amounts within a given MPN dilution after growth.
[b]Grew in the presence or absence of 2M NaCl.
[c]Grew only in the absence of 2M NaCl.
[d]Grew only in the presence of 2M NaCl.

greatly appreciated. This project was supported by the NASA-ASTEP grants SOTF NNG04-GB66G and LITA NAG5-12890.

References

Amman, R., W. Ludwig, and K. Schleifer (1995), Phylogenetic identification and in situ detection of individual microbial cells without cultivation, *Microbiol. Rev.*, *59*, 143–169.

Cabrol, N. A., et al. (2007), Life in the Atacama: Searching for life with rovers (science overview), *J. Geophys. Res.*, doi:10.1029/2006JG000298, in press.

de Man, J. C. (1975), The probability of most probable numbers, *Eur. J. Appl. Microbiol.*, *1*, 67–78.

Dohm, J. M., et al. (2005), Life in the Atacama - Year 2: Geologic reconnaissance through long-range roving and implications on the search for life, *Proc. Lunar Planet. Sci. Conf.*, *XXXVI*, Abstract 1579.

Drees, K., J. Neilson, J. Betancourt, J. Quade, D. Henderson, B. Pryor, and R. Maier (2006), Bacterial community structure in the hyperarid core of the Atacama Desert, Chile, *Appl. Environ. Microbiol.*, *72*(12), 7902–7908.

Dunai, T., and G. A. González-López (2005), Oligocene-Miocene age of aridity in the Atacama Desert revealed by exposure dating of erosion-sensitive landforms, *Geology*, *33*(4), 321–324.

Edwards, D., T. Rogall, H. Blocker, M. Emde, and E. C. Bottger (1989), Isolation and direct complete nucleotide determination of entire genes: Characterization of a gene coding for ′16S ribosomal RNA, *Nucleic Acids Res.*, *17*, 7843–7853.

Ericksen, G. (1983), The Chilean nitrate deposits, *Am. Sci.*, *71*, 366–375.

Ewing, S., B. Sutter, J. Owen, K. Nishiizumi, W. Sharp, S. Cliff, K. Perry, W. Dietrich, C. P. McKay, and R. Amundson (2006), A threshold in soil formation at the arid-hyperarid transition on Earth, *Geochem. Cosmochem. Acta*, *70*, 5293–5322.

Fay, H. (1982), Method and apparatus for detecting fluorescence under ambient light conditions, *United States Patent 4*, *336*, 459.

Ford, M. A., and B. B. Leather (1984), Minimizing the effect of spurious photodetector currents in flash spectrofluorimetry, *United States Patent 4*, *438*, 329.

Friedmann, E. I., and M. Galun (1974), Desert algae, lichens and fungi, in *Desert Biology*, edited by G. Brown, pp. 165–212, Academic, New York.

Hartmann, A., B. Assmus, G. Kirchoff, and M. Schloter (1997), Direct approaches for studying soils microbes, in *Modern Soil Microbiology*, edited by J. van Elsas, J. Trevors, and E. Wellington, pp. 279–309, Dekker, New York.

Houston, J., and A. Hartley (2003), The central Andean west-slope rainshadow and its potential contribution to the origin of hyper-aridity in the Atacama Desert, *Int. J. Climatol.*, *23*, 1453–1464.

Hughes, J., J. Hellmann, T. Ricketts, and B. Bohannan (2001), Counting the uncountable: Statistical approaches to estimating microbial diversity, *Appl. Environ. Microbiol.*, *67*(10), 4399–4406.

Kaeberlein, T., K. Lewis, and S. Epstein (2002), Isolating "uncultivable" microorganisms in pure culture in a simulated natural environment, *Science*, *296*, 1127–1129.

Kim, M., A. Lefcourt, and Y. R. Chen (2003), Multispectral laser-induced fluorescence imaging system for large biological samples, *Appl. Opt.*, *42*, 3927–3934.

Latorre, C. (2002), Clima y Vegetación del Desierto de Atacama Durante el Cuaternario Tardío, II Región, Chile, Ph.D. dissertation, Univ. de Chile, Santiago.

Latorre, C., J. L. Betancourt, K. A. Rylander, J. Quade, and O. Matthei (2003), A vegetation history from the arid prepuna of northern Chile (22–23°S) over the last 13,500 years, *Palaeogeogr. Palaeoclimatol. Palaeoecol.*, *3064*, 1–25.

Lester, E., M. Satomi, and A. Ponce (2007), Microflora of extreme arid Atacama Desert soils, *Soil Biol. Biochem.*, *39*, 704–708.

Li, Y., W. Kick, and O. Tuovinen (2004), Fluorescence microscopy for visualization of soil microorganisms—A review, *Biol. Fertil. Soils*, *39*, 301–311.

Lloyd-Jones, G., and D. Hunter (2001), Comparison of rapid DNA extraction methods applied to contrasting New Zealand soils, *Soil Biol. Biochem.*, *33*, 2053–2059.

Maidak, B. L., et al. (2000), The RDP (Ribosomal Database Project) continues, *Nucleic Acids Res.*, *28*, 173–174.

McKay, C. P., E. I. Friedmann, B. Gómez-Silva, L. Cáceres, D. Andersen, and R. Landheim (2003), Temperature and moisture conditions in the extreme arid regions of the Atacama Desert: Four years of observations including the El Niño of 1997–98, *Astrobiology*, *3*, 393–406.

Miller, A. (1976), The climate of Chile, in *World Survey of Climatology*, vol. 12, *Climates of Central and South America*, edited by R. Schwerdtfeger, pp. 113–145, Elsevier Sci., Amsterdam.

Miller, D., U. Bryant, and E. Madsen (1999), Evaluation and optimization of DNA extraction and purification procedures for soil and sediment samples, *Appl. Environ. Microbiol.*, *65*, 4715–4724.

NASA (2006), NASA Mars Exploration Program, Program Plan, December 2006, *JPL Doc.*, *D-23969*.

Navarro-González, R., et al. (2003), Mars-like soils in the Atacama Desert, Chile, and the dry limit of microbial life, *Science*, *302*, 933–1096.

Nienow, J., and E. I. Friedmann (1993), Terrestrial lithophytic (rock) communities, in *Antarctic Microbiology*, edited by E. I. Friedmann, pp. 243–412, Wiley-Liss, New York.

Norikane, J. H., and K. Kurata (2001), Water stress detection by monitoring fluorescence of plants under ambient light, *Trans. ASAE*, *44*, 1915–1922.

Piatek, J. L., et al. (2005), Spectroscopic results from the Life in the Atacama (LITA) project 2004 field season, *Proc. Lunar Planet. Sci. Conf.*, *XXXVI*, Abstract 1563.

Quinn, R., A. Zent, F. Grunthaner, P. Ehrenfreund, C. Taylor, and J. Garry (2005), Detection and characterization of oxidizing acids in the Atacama Desert using the Mars Oxidation Instrument, *Planet. Space Sci.*, *53*, 1376–1388.

Rech, J., J. Quade, and W. Hart (2003), Isotopic evidence for the source of Ca and S in soil gypsum, anhydrite and calcite in the Atacama Desert, Chile, *Geochim. Cosmochim. Acta*, *67*, 575–586.

Riquelme, R., J. Martinod, G. Hérail, J. Darrozes, and R. Charrier (2003), A geomorphological approach to determining the Neogen to recent tectonic deformation in the coastal cordillera of northern Chile (Atacama), *Tectonophysics*, *361*, 255–275.

Rundel, P., M. Dillon, B. Palma, H. Mooney, S. Gulman, and J. Ehleringer (1991), The phytogeography and ecology of the coastal Atacama and Peruvian deserts, *Aliso*, *13*, 1–49.

Shapiro, H. M. (2003), *Practical Flow Cytometry*, John Wiley, Hoboken, N. J.

Sutter, B., R. Amundson, S. Ewing, K. Warren-Rhodes, and C. McKay (2002), The chemistry and mineralogy of Atacama Desert soils: A possible analog for Mars soils, *Eos Trans. AGU*, *83*(47), Fall Meet. Suppl., Abstract P71A-0443.

Tien, C., C. Chao, and W. Chao (1999), Methods for DNA extraction from various soils: A comparison, *J. Appl. Microbiol.*, *86*, 937–943.

Warren-Rhodes, K. A., K. Rhodes, S. Pointing, S. Ewing, D. Lacap, B. Gómez-Silva, R. Amundson, E. I. Friedmann, and C. P. McKay (2006), Hypolithic cyanobacteria, dry limit of photosynthesis and microbial ecology in the hyperarid Atacama Desert, *Microb. Ecol.*, *52*, 389–398.

Warren-Rhodes, K. A., et al. (2007), Robotic ecological mapping: Habitats and the search for life in the Atacama Desert, *J. Geophys. Res.*, doi:10.1029/2006JG000301, in press.

Weinstein, S., et al. (2005), Use of a novel rover-mounted fluorescence imager and fluorescent probes to detect biological material in the Ataca-

ma Desert in daylight, *Proc. Lunar Planet. Sci. Conf.*, *XXXVI*, Abstract 1494.

Wettergreen, D. S., N. A. Cabrol, J. Teza, P. Tompkins, C. Urmson, V. Verma, M. Wagner, and W. Whittaker (2005), First experiment in the robotic investigation of life in the Atacama Desert of Chile, paper presented at EEE International Conference on Robotics and Automation (ICRA), Barcelona, May.

Zengler, K., G. Toledo, G. Rappé, J. Elkins, E. Mathur, J. Short, and M. Keller (2002), Cultivating the uncultured, *PNAS*, *99*(24), 15,681–15,686.

D. Apostolopoulos, G. G. Oril, T. Smith, K. Stubbs, M. Wagner, and D. S. Wettergreen, Robotics Institute, Carnegie Mellon University, Pittsburgh, PA 15213, USA.

N. A. Cabrol and E. Grin, SETI Institute, Mountain View, CA 94043, USA.

C. Cockell, Planetary and Space Sciences Research Institute, Open University, Milton Keynes MK7 6AA, UK.

P. Coppin, Eventscope, Carnegie Mellon University, Pittsburgh, PA 15213, USA.

C. Diaz, Universidad Católica del Norte, 0610 Antofagasta, Chile.

J. Dohm and M. Wyatt, Department of Hydrology and Water Resources, University of Arizona, Tucson, AZ 85721, USA.

S. Emani, L. A. Ernst, G. Fisher, E. Minkley, D. Pane, A. S. Waggoner, and S. Weinstein, Molecular Biosensor and Imaging Center, Carnegie Mellon University, Pittsburgh, PA 15213, USA.

A. Hock, Department of Earth and Space Sciences, University of California, Los Angeles, CA 90095, USA.

J. Moersch and J. Piatek, Department of Earth and Planetary Sciences, University of Tennessee, Knoxville, TN 37996, USA.

G. Thomas, Department of Mechanical and Industrial Engineering, University of Iowa, Iowa City, IA 52242, USA.

K. Warren-Rhodes, NASA Ames Research Center, MS 245-3, Moffett Field, CA 94035, USA. (kwarren-rhodes@mail.arc.nasa.gov)